

J. Klahold, J. Rautenberg, and U. Rückert. Ultrasonic Sensor for Mobile Mini-Robots Using Pseudo-Random Codes. In *Proceedings of the 5th International Heinz Nixdorf Symposium: Autonomous Minirobots for Research and Edutainment (AMiRE)*, volume 97 of *HNI-Verlagsschriftenreihe*, pp. 225–232, 2001.

Ultrasonic Sensor for Mobile Mini-Robots Using Pseudo-Random Codes

J. Klahold, J. Rautenberg, and U. Rückert

System and Circuit Technology, Heinz Nixdorf Institute,
Paderborn University, Fürstenallee 11, D-33102 Paderborn

E-mail: klahold@hni.uni-paderborn.de

Abstract. Ultrasonic sensors enable mobile autonomous systems to obtain information about obstacles in large environments. In the presented work, taking the limited energy resources of a mobile robot into account, only one transmitter is used. The employment of two receivers permits the calculation of the distance and direction of objects. Using pseudo-random sequences, simultaneously transmitting and receiving with the continuous perception of the environment is possible. The sequences are modulated in order to optimise the signal-to-noise ratio and energy consumption with respect to the transducers' bandwidth. With the gained signals the echo-intensity field is calculated for object detection. Furthermore, several robots could operate in the same region applying orthogonal sequences.

1 Introduction

Recognising the environment is substantial for all autonomous systems. Therefore sensors have to meet several requirements. They should enable real-time perception of the environment and cover a large scope with high resolution, taking the provided computing power for information processing and the limited energy resources of a small autonomous robot into account. Regarding these limitations, the evaluation of ultrasonic echos is an excellent way for perceiving the environment.

Using one transducer, only a one-dimensional perception [8] is possible. The employment of several transducers permits more exact perception. Kleeman and Kuc [6] use two transmitters and two receivers in order to distinguish characteristics, e.g. walls, corners and edges. Klahold et al [5] show that two receivers are needed to obtain the distance and direction of an object. One additional transmitter enables simultaneous sending and receiving. This arrangement can be observed in nature e.g. in bats. The ultrasonic wave sent out by a bat, consists of two components. One with a constant frequency of about 75 kHz and a duration of about 40 ms followed by another with a modulated frequency lasting 2 ms [11]. The evaluation of the incoming signal is split into an inter-aural intensity and time difference respectively [7]. This paper only considers the evaluation of the time differences and intensity levels.

This principle of measuring the time-of-flight of a burst with a fixed frequency is conventionally used for an ultrasound based distance estimation. Applying a burst of pseudo-random frequencies, the signal-to-noise ratio (SNR) is maximised [4]. It also increases the angular and range

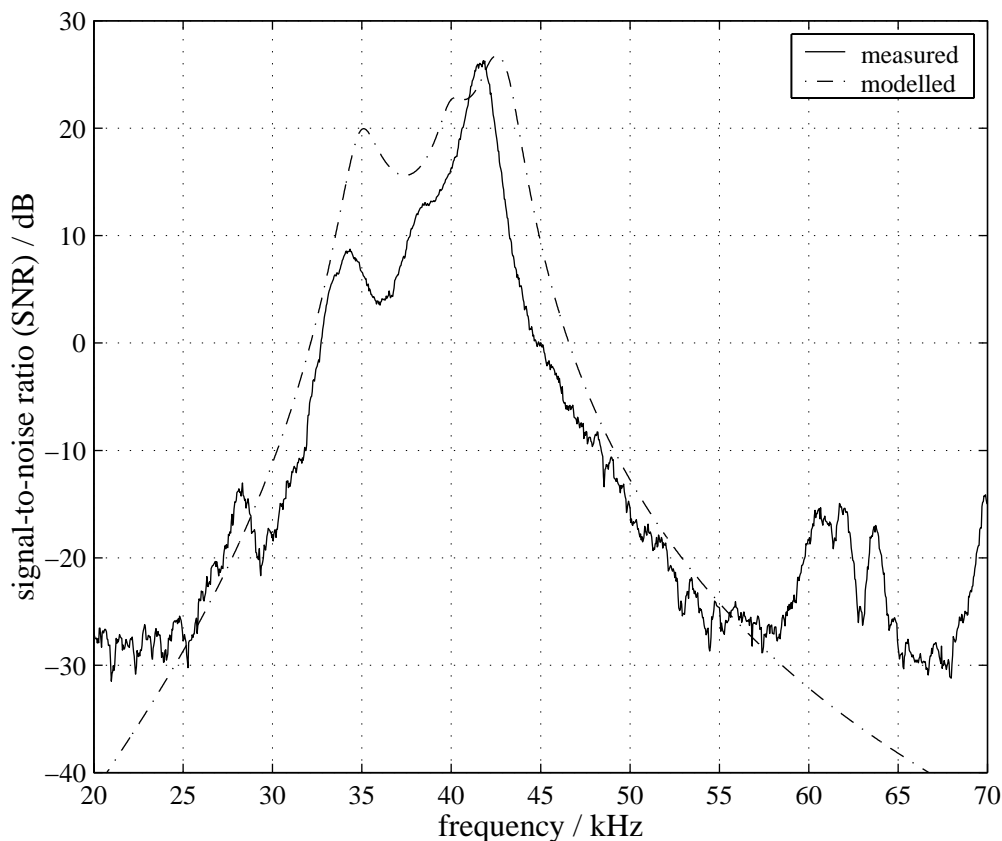


Figure 1. Transferfunction of the transducers with a distance of 30 cm between transmitter and receiver.

resolution and minimises misreadings due to either external ultrasound sources or crosstalk [2]. For applications with several robots, it is useful, if each one can identify both, echo signals and signals of other robots. This could also be a basis for communication. Considering mobile phones, m-sequences or gold-codes can be used as pseudo-random numerical sequences [9]. These pseudo-random signals must have good correlation properties to enable time-of-flight measuring.

This paper is organised as follows: First, there is an introduction to the used hardware in section 2, followed by a description of signal processing in section 3. Finally, there is the discussion of the results in section 4 and a summary with an outlook in section 5.

2 Hardware Platform

This section describes the hardware of the sensor module which gives restrictions to the signal-generation and resolution. The Polaroid “L”-Series 10LT40 and 10LR40 [13], with a centre frequency of 40 kHz, are used as transducers. The Bandwidth (Fig. 1) is tuned to about 25 kHz with a resistor and an inductance in series to the transmitter and parallel to the receiver respectively [10]. The transducers are connected to the K-Flex-FPGA-Board [12] with a Xilinx 4044 field-programmable gate array (FPGA) via amplifier, antialiasing filter and analog-digital converter or driver respectively (Fig. 2(a)).

In this first version of the module only the sequence generation, the dynamic simulation and the

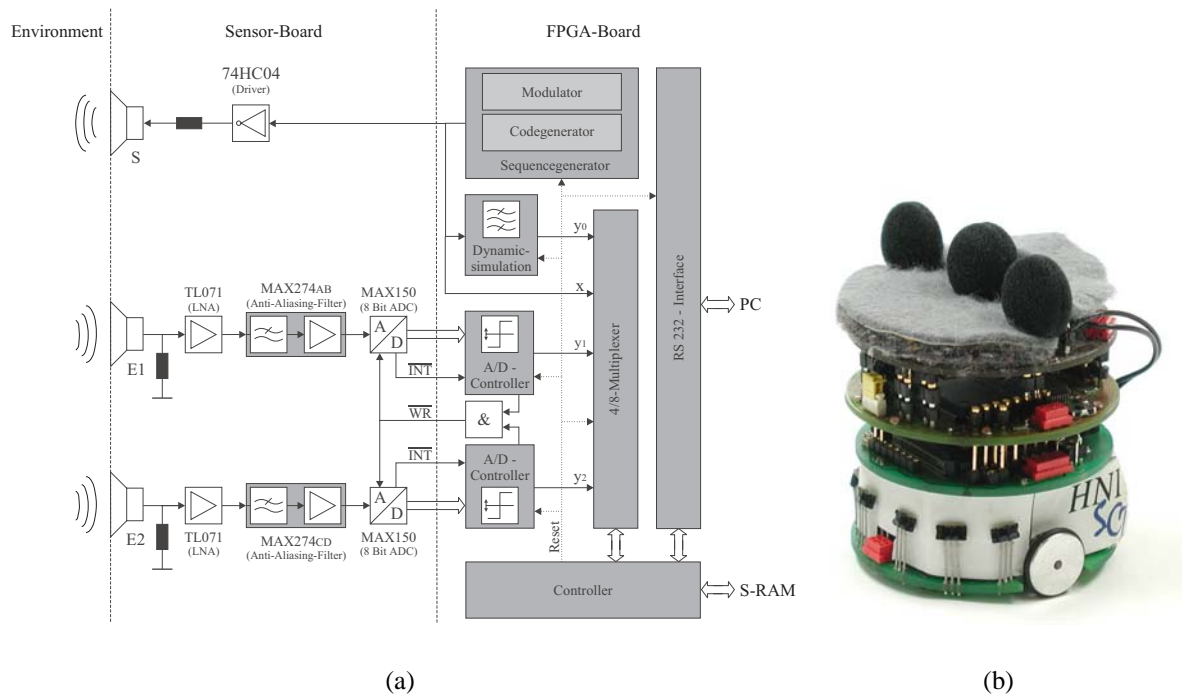


Figure 2. Schematic of the ultrasonic sensor module (a) and the Khepera with the module (b).

controllers are realized as digital components in the FPGA. The dynamic simulation—Finite Impulse Response (FIR) filter of 56th order—generates a reference signal (y_0 in Fig. 2(a)) with respect to an empty environment-channel for the correlation. This economises an additional receiver generating a reference signal. The A/D-Controllers are used as triggers with dynamic thresholds, preprocessing a mean-less signal for dual-switched-correlation, which is no limitation for time-of-flight measurements however reduces hardware requirements. The gained signals are stored in the SRAM of the K-Flex-FPGA-Board. On request they are transferred to a PC for correlation and analysis.

The mini-robot Khepera [3] is used as the mobile platform. Due to its small size—diameter of 5.5 cm—the transducers have to be placed closely together. The receivers are arranged, with consideration to the nature of bats, in equal distances to the left and right of the transmitter. This is no general limitation [5], but the angular-resolution increases by distance between the receivers (q) (Eqn. 5). A decreasing, direct sound-component increases the range. Figure 2(b) shows the robot with the ultrasonic module.

3 Signal Processing

To optimise the perception, the generated pseudo-random signal should have a sharp autocorrelation function with no two arbitrary sequences correlating [9]. A Gold-Code, generated from two shift-registers with a length of 9, is used as the pseudo-random sequence. Therewith, the autocorrelation has a maximum of $2^9 - 1 = 511$ while the cross-correlation could only result in -1, -33 or 31.

Due to the limited bandwidth and the centre-frequency of the ultrasonic transducers, the pseudo-random sequence spectrum has to be shifted. It is important that the correlation properties

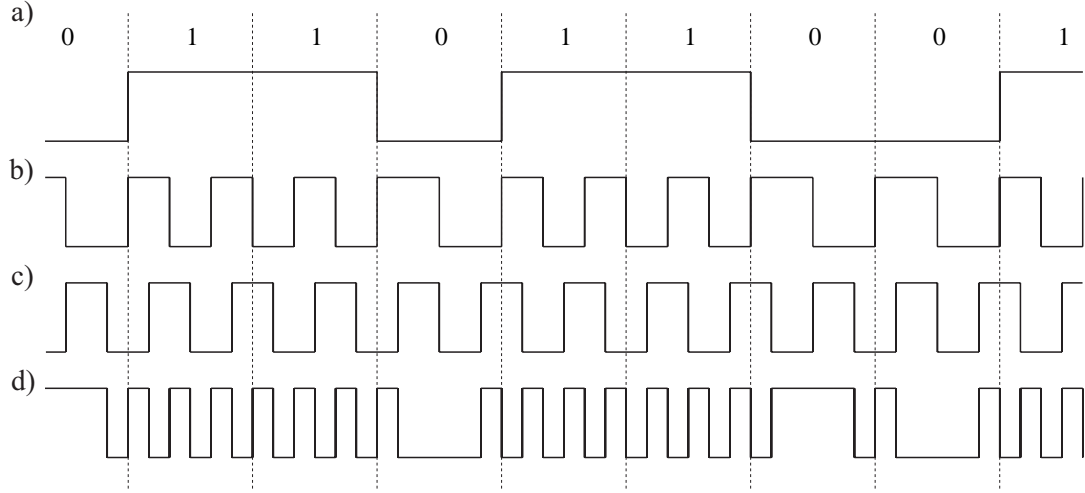


Figure 3. Illustration of the modulation: a) unmodulated pseudo-random sequence, b) Minimum-Shift-Keying (MSK)—Frequency-Modulation (FM) with sequence-conducted change of ranks, c) carrier with odd division for Phase-Modulation (PM), d) MSK-PM signal (XOR of b and c).

do not change and that as much energy as possible is transmitted. Therefore, we choose a combination of a Minimum-Shift-Keying (MSK) and a rectangular Phase-Modulation (PM). Figure 3 shows the generation of the transmitted signal. The sequence has a symbol-frequency (f_s) of approximately 14.6 kHz (Fig. 3(a)). The generated MSK-PM signal has approximately a centre-frequency (f_c) of 40.2 kHz and a bandwidth (B) of 25.6 kHz. Figure 4 shows the auto- and cross-correlation of such modulated sequences.

The velocity of sound in air is assumed to be $c = 343 \text{ m/s}$. With a sequence-length (N) of 511 one cycle covers $c \cdot N/f_s \approx 12 \text{ m}$ which ensures unambiguous operation of up to approximately 6 m. For an accurate reconstruction of the signal we choose a sample-frequency ($f_a = T_a^{-1} = 24 \cdot f_s$) of 351 kHz. The sequence is continuously transmitted and simultaneously received, which ensures an uninterrupted perception. Similar to the sense of vision of humans it is possible to evaluate an average impression of the environment ($f_s/N \approx 28.6$ cycles per second).

Only the sign bit of each signal (x , y_0 , y_1 and y_2 in Fig. 2(a)) is recorded and transferred to a PC. This ensures flexible operation and evaluation of several algorithms. In a future version, correlation and object detection will be implemented in the FPGA. Therefore, all algorithms are kept as simple as possible.

In the first step of the analysis the received signals—from the left and right transducer—are correlated with the reference signal. Assuming a simple model of the channel with multiple echos and their different attenuation (D_i) the cross-correlation results in:

$$\Phi_{y_0 y_1}(\tau) = \sum_{i=0}^{24 \cdot N} D_{1i} \cdot \Phi_{y_0 y_0}(\tau - i T_a) \quad (1)$$

$$\Phi_{y_0 y_2}(\tau) = \sum_{i=0}^{24 \cdot N} D_{2i} \cdot \Phi_{y_0 y_0}(\tau - i T_a) \quad (2)$$

This step is repeated with every new sample approximating an average cross-correlation. The result is smoothed (Fig. 5(a)) with a \cos^4 -window which has a width of 1.5 cm corresponding

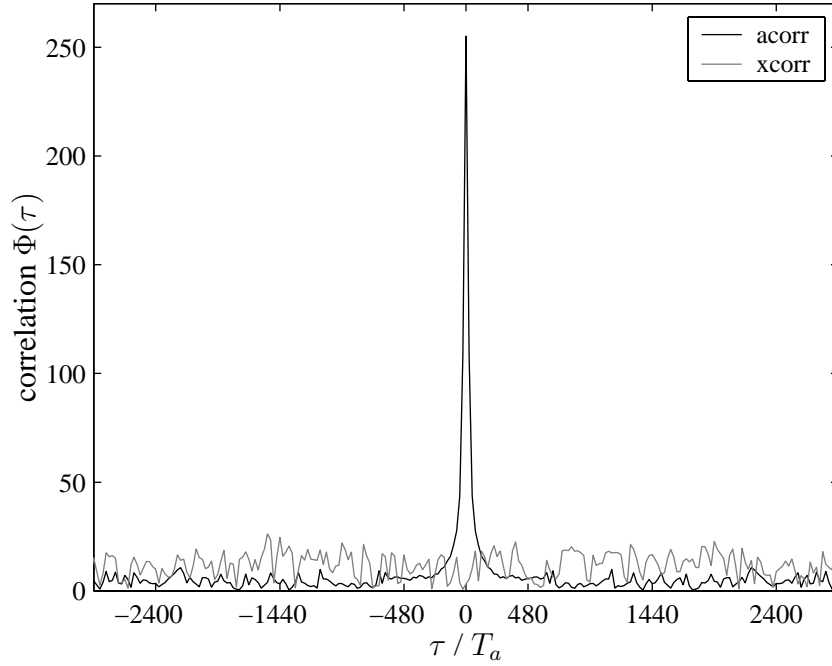


Figure 4. Auto- (acorr) and cross-correlation (xcorr) of MSK-PM modulated pseudo-random sequences.

to the width of the autocorrelation. The direct component is suppressed by subtraction so that close objects can be detected as well.

Maxima above a threshold (dashed line) indicate an object at a certain distance. In order to determine the direction where the object resides, both signals are combined to an array. Thereby, all possible correspondences between y_1 and y_2 are covered by the time-of-flight difference $\Delta\tau$ and all possible distances are covered by the average time-of-flight τ . The result is a matrix $\tilde{\Phi}(\tau, \Delta\tau)$ (Eqn. 3).

$$\tilde{\Phi}(\tau, \Delta\tau) = \Phi_{y_0y_1} \left(\tau + \frac{\Delta\tau}{2} \right) \cdot \Phi_{y_0y_2} \left(\tau - \frac{\Delta\tau}{2} \right) \quad (3)$$

Regarding the chosen sensor arrangement the matrices for the conversion from time-of-flight to the cylindrical polar coordinates (ρ, φ) result in:

$$\rho = \frac{c^2\tau^2 + \frac{c^2}{4}\Delta\tau^2 - \frac{q^2}{4}}{2c\tau} \quad (4)$$

$$\sin(\varphi) = \frac{c}{q} \Delta\tau \left(\frac{2c^2\tau^2}{c^2\tau^2 + \frac{c^2}{4}\Delta\tau^2 - \frac{q^2}{4}} - 1 \right) \quad (5)$$

This array $\tilde{\Phi}(\rho, \varphi)$ (Fig. 5(b)) can be seen as the echo-intensity field. The maximum regions of the field corresponding to the maxima of the correlation are extracted for further classification.

Utilising the gained D_i , a "target-strength" is calculated with respect to the absorption of air [1] and an additional dependence of the distance (ρ^{-4}). This is used to calculate the size of objects. Furthermore, the directional characteristic of the transducers will be considered so that sidewise placed objects are valued more strongly. It is assumed that only walls are potential objects. These walls are drawn orthogonally to the location-vector of the maximum in the map (Fig. 5(c)). Their size corresponds to the target-strength. Smaller objects are supposed to be measurement errors.

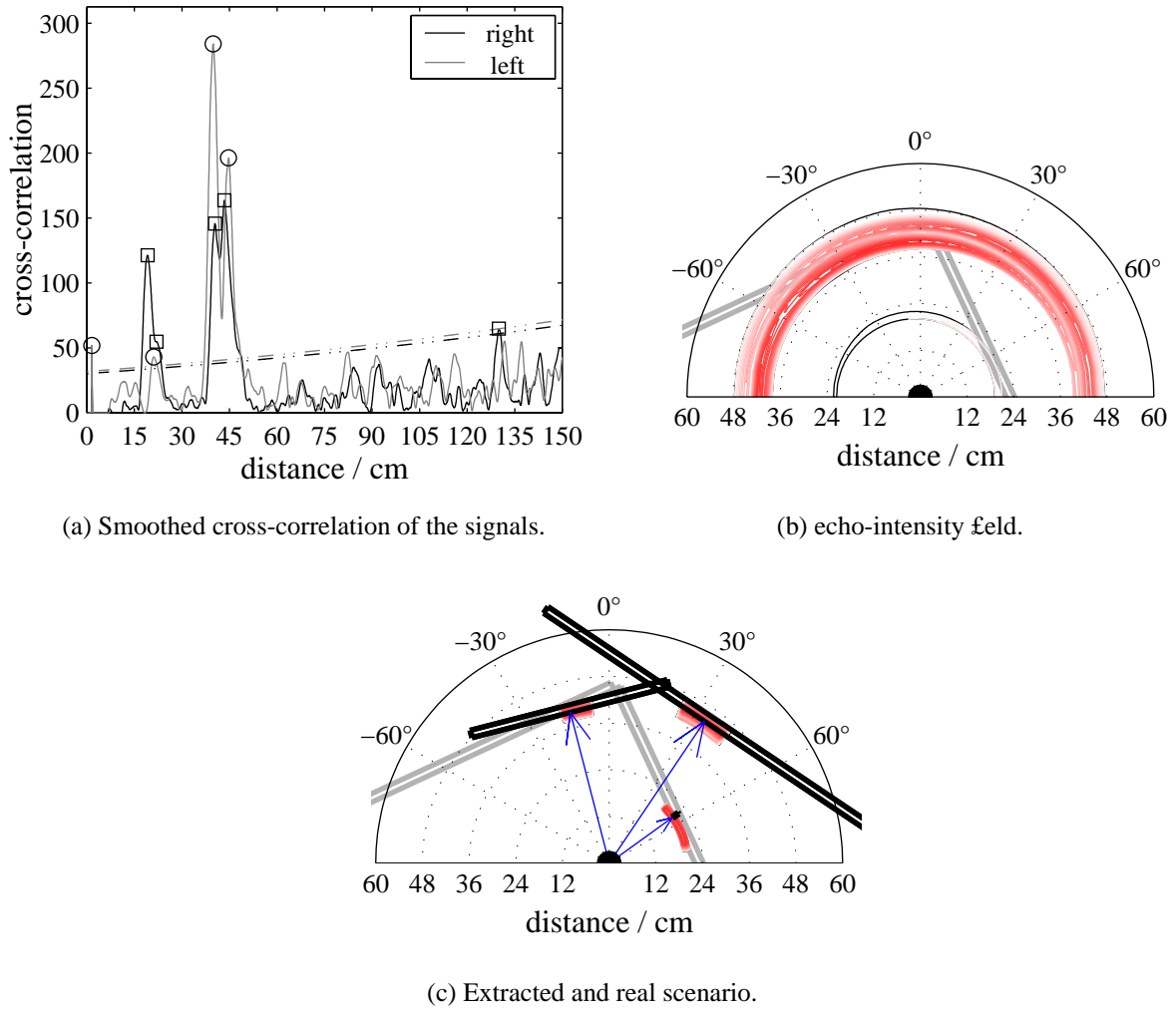


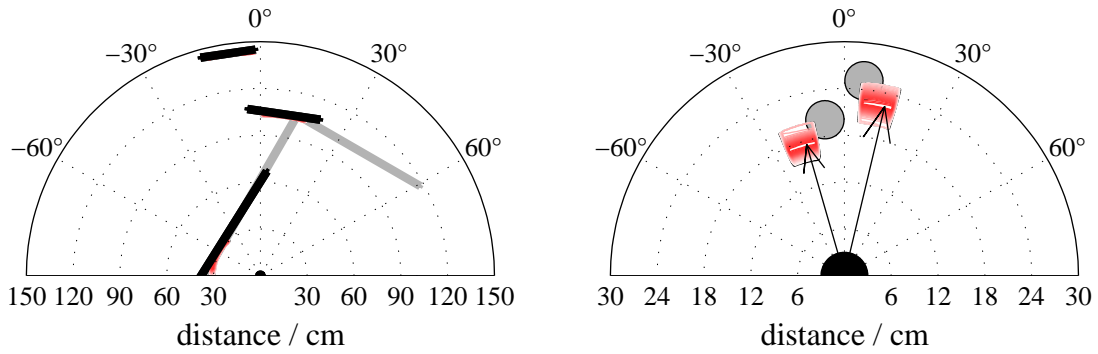
Figure 5. Example of the object perception. The system is fronted to a corner. Three walls are detected—one is a phantom caused by multiple reflection.

4 Results

Theoretically, the system can discriminate 101 angles over 180° and distances with an accuracy of ± 0.73 mm. The perception decreases from the front of the robot to the sides. Reliable information can be gained in a sector of $\pm 60^\circ$ up to about 1 m. For verification of the results, the images show the original placement of the objects in grey, the relevant echo-intensity field and the calculated walls in black. Alignment errors are mainly caused by unprecise robot position.

Illustrating the capabilities of the system some examples are shown. The first example (Fig. 5(c)) shows the robot targeted to a corner, recognised as two walls. Further on a third wall which is a phantom of the left wall caused by multiple reflection, is detected. Identifying such phantom-objects requires advanced considerations which are not yet realized.

Figure 6(a) demonstrates the perception of a wall under an angle of 60° on the left. Additionally, the corner and a phantom of the right wall are drawn. An example for the differential capabilities is the image with the two barrels (Fig. 6(b)). It should be noted that the barrels are located at the outer margins of their real places. In the last illustration a 1.25 mm thick wire is shown in



(a) Extreme situation: a wall under -60° .

(b) Perception of closely placed barrels.

Figure 6. Two examples demonstrating the capabilities of the system.

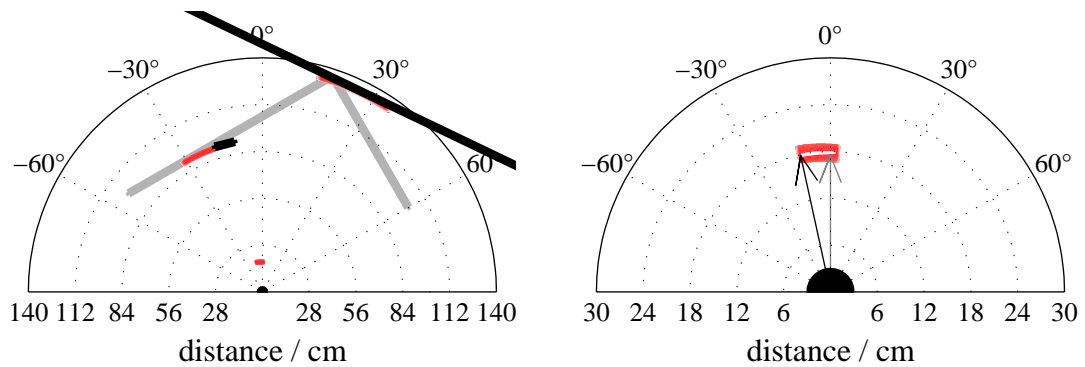


Figure 7. Perception of a 1.25 mm thick wire. On the right a detailed view of the wire is shown.

front of a corner (Fig. 7). Note that this is 6.9 times smaller than the wavelength ($\lambda = 8.6$ mm).

5 Conclusions

This paper shows the development of a new ultrasonic module for small autonomous mobile robots, e.g. the mini-robot Khepera. The covered area enlarges the perception-space of such a small robot and still provides information about near, small obstacles. The sound is transmitted continuously so that an uninterrupted perception is possible. By using pseudo-random sequences, e.g. Gold-Codes, several robots with orthogonal codes could operate in the same region. The knowledge of codes from other robots will permit communication between each other. Furthermore, the tracking of other robots is possible and thus an alignment of their positions.

References

- [1] H. E. Bass, L. C. Sutherland, A. J. Zuckerwar, D. T. Blackstock, and D. M. Hester. Atmospheric absorption of sound: Further developments. *Journal of the Acoustical Society*

of America, 97(1):680–683, 1995.

- [2] **K.-W. Jörg** and **M. Berg**. Sophisticated mobile robot sonar sensing with pseudo-random codes. *Robotics and Autonomous Systems*, 25(3–4):241–251, 1998.
- [3] **K-Team S.A.** Products: Mobile Robots. <http://www.k-team.com/products.html>, 2000. last visit May 2001.
- [4] **W. K. Kim**, **S. B. Park**, and **S. A. Johnson**. Signal-to-noise ratio and bandwidth for pseudo-random codes in an ultrasonic imaging system. *Ultrasonic Imaging*, 6:313–323, 1984.
- [5] **J. Klahold**, **A. Löfner**, and **U. Rückert**. Discrete Ultrasonic Sensors for Mobile Autonomous Systems. In *Proceedings of the 1st International Khepera Workshop*, volume 64 of *HNI-Verlagsschriftenreihe*, pp. 171–180, 1999.
- [6] **L. Kleeman** and **R. Kuc**. Mobile Robot Sonar for Target Localization and Classification. *The International Journal of Robotics Research*, 14(4):295–318, 1995.
- [7] **A. Kleiser**. *Antwortverhalten von Neuronen des Colliculus inferior auf bewegte Schallreize bei der Fledermaus *Rhinolophus rouxi**. PhD thesis, Ludwig-Maximilians-Universität München, 1997.
- [8] **J. J. Leonard** and **H. F. Durrant-Whyte**. *Directed Sonar Sensing for Mobile Robot Navigation*. Kluwer Academic Publishers, 1992.
- [9] **H. D. Lüke**. *Korrelationssignale*. Springer, 1992.
- [10] **Massa**. Products Corporation – Model E-152. <http://www.massa.com/datasheets/e152.html>, 2000. last visit May 2001.
- [11] **G. Neuweiler**. *Biologie der Fledermäuse*. Thieme, 1993.
- [12] **J.-C. Niemann**, **U. Witkowski**, **M. Porrmann**, and **U. Rückert**. Extension Module for Application Specific Hardware on the Mini Robot Khepera. In *Proceedings of the 5th International Heinz Nixdorf Symposium: Autonomous Minirobots for Research and Entertainment*, HNI-Verlagsschriftenreihe, 2001.
- [13] **Polaroid**. Products: Ultrasonics. <http://www.polaroid-oem.com/products/ultrasonic.htm>, 2000. last visit May 2001.